Effective Prandtl Number, Hall Currents, Soret, and Dufour Effect on MHD Flow Past an Inclined Stretching Sheet with Aligned Magnetic Field and Heat Generation

George Buzuzi, Martin T Kudinha, William M Manamela

Abstract—Numerical study of steady MHD convective flow of viscous incompressible electrically conducting fluid over an inclined stretching surface with aligned magnetic field, Hall effect, effective Prandtl number and heat generation is carried out. The partial differential equations are transformed to a system of non-linear ordinary differential equations which are then solved numerically by MATLAB bvp4c solver. The profiles of the velocity, temperature and concentration are analysed and duscussed with the numerical results presented graphically. The calculated values of skin-friction, the heat transfer rate and mass transfer rate at the surface are discussed numerically for various values of the physical parameters and tabulated. Results reveal that for attainment of optimal velocity profile, the amount of inclination of the magnetic field and the stretching surface need to be relatively small and that for a given effective Prandtl number the value of the Prandtl number should be greater than that of the radiation parameter.

Index Terms: **MHD, aligned magnetic field, inclined sheet, effective Prandtl number, Hall current.**

I. INTRODUCTION

THE study of magnetohydrodynamic(MHD) flow has significant applications in agriculture, engineering, petroleum industries, plasma studies, cooling of nuclear reactors and aerodynamics (see[28], [5], among others)

The impact of thermal radiation on MHD fluid is important under various isothermal and non-isothermal environments. For instance, radiation plays a pivotal role in polymer extrusion process under controlled thermal environment. The characteristics of the end product in a system is controlled by one's knowledge of radiation heat transfer. The transfer of heat through radiation has various applications. In nuclear and industrial engineering it plays a vital role in the design of satellites and aircraft missiles propulsion devices. The role of thermal radiation has been studied by many researchers, notably among them, Seddeeck and Muguid [27], Ibrahim *et al.* [14] and Roja *et al.* [22]. Following studies carried out by Buzuzi [9], Mgyari [17] and Magyari and Pantokratoras [18], it has been shown that the impact of thermal radiation in the linearized Rosseland approximation is insignificant since its effect is not different from that of the Prandtl number except that the magnitude of the impact is re-scaled. Further in their analysis, the same researchers observed that solutions involving the radiation parameter in linearized Rosseland approximation is a function of both the radiation parameter and the Prandtl number, called the effective Prandtl number. The present study is a case in point where we investigate the combined effect of the two parameters, the radiation parameter R and the Prandtl number P_r.

Many studies on MHD flow over surfaces involve normal magnetic field. However, due to some geometry limitations in some manufacturing processes, the magnetic field maybe applied obliquely to the surfaces. Consequently, considerable progress has been made in the study of aligned magnetic field. Several authors who include Salawa and Dada [24], Snrini-vasulu *et al.* [30], Acharya *et al.* [2], Devi *et al.* [11], Sandeep and Sugunamma [26], Raju *et al.* [20] and Buzuzi [9] have studied the influence of aligned magnetic field and found that increasing the magnetic field angle of inclination, improves the heat transfer rate, strengthens the magnetic field and reduces the velocity profile.

The flow of fluid past inclined surfaces has attracted the attention of many authors, among them are, Buzuzi *et al.* [6], Alam *et al.* [3], Uddin [33], Alam *et al.* [4], Buzuzi and Buzuzi [7], Titus *et al.* [32], Buzuzi *et al.* [8], Vijayaragavan *et al.* [35], Buzuzi [9] and Shoaib *et al.* [29]. Their findings showed that increasing the inclination of the flow surface enhances the temperature profile and diminishes the velocity profile.

Studies by Shateyi *et al.* [28], Sabhakar *et al.* [23] and Gajjela *et al.* [13] revealed that the rate of energy transfer is generated by composition gradient or temperature gradient. The mass fluxes caused by temperature gradients are called thermal-diffusion effect or Soret effect. The energy flux which is caused by composition gradient is known as diffusion-thermo effect or Dufour effect. Most of the above referenced work considered Dufour and Soret effects insignificant compared to the effects explained by Fourier's

law.

Electrical conductivity is influenced by the presence of a magnetic field and a strong electric field. The current flows in the direction perpendicular to both the magnetic field and the electric field, a phenomenon called Hall effect(Cowling [10], Shateyi *et al.* [28], Kishna *et al.* [16], among others). In this study, a strong magnetic field is subjected to the fluid flow and thus the Hall effect cannot be ignored, which has considerable impact on the current density and the magnetic force. The Hall effects on MHD fluid flow have many engineering applications in electric transformers, MHD accelerators, heating elements and power generators (see[Salem and Aziz [25], Shateyi *et al.* [28], Krishna and Jyothi [15]], among others. The influence of Hall currents on MHD flow past a moving flat plate was investigated by Watanabe and Pop [34]. Abo-Eldahab and Salem[1] investigated Hall impact of Hall on non-Newtonian MHD power-law fluid. The study of MHD fluid flow over a vertical plate with varying temperature and mass diffusion and Hall currents was analysed by Rajput and Kanaujia[19]. Krishna and Kyoto [15] studied the influence of heat source, chemical reaction, and Hall effects of visco-elastic fluid past an infinite oscillating porous plate.

In the majority of these Hall effect studies, the researchers investigated fluid flow involving either aligned magnetic field or inclined flow surface but not both. Only a few authors have analysed the effect of both aligned magnetic field and inclined flow surface. Reddy *et al.* [21], Sivaraj and Sheremet [31] are some of the researchers who investigated the influence of both inclined flow channel and magnetic field inclination angle. Most recently, Buzuzi and Buzuzi [7] and Buzuzi [9] considered the combined effect of the flow surface inclination and aligned magnetic field. However their analysis did not involve the effective Prandtl number, Hall currents, Dufour and Soret effects. The current study extends the work of Shateyi *et al.* [28] by introducing an aligned magnetic field, inclined flow surface, heat generation parameter and the effective Prandtl number.

According to the authors' knowledge, there are no studies reported so far on the influence of the effective Prandtl number, Hall currents, Dufour effects and Soret effects on MHD flow subjected to aligned magnetic field, heat generation and inclined stretching sheet.

The succeeding sections of this paper are as follows. The problem formulation is found in section 2 and the method of solution is presented in section 3. Results and discussion of the results are covered in section 4 and lastly section 5 gives the concluding remarks.

II. MATHEMATICAL ANALYSIS

Consider a steady MHD fluid flow subjected to aligned magnetic field, effective Prandtl number, Soret effect, Dufour effect, Hall currents, heat generation, and inclined stretching surface.
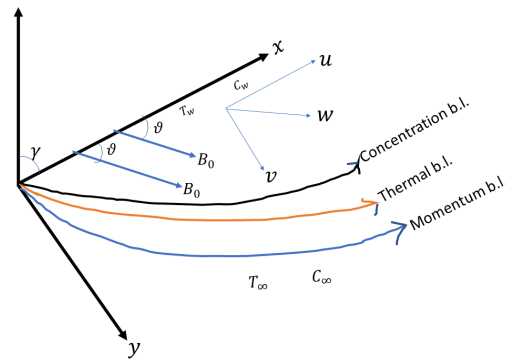

Figure 1:Flow geometry

The flow configuration and coordinate system are depicted in Figure 1 where the $x-$axis is directed parallel to the plate and the $y-$ axis is directed perpendicular to it. The flow surface is at an angle γ from the vertical direction. The magnetic field of strength B_0 is inclined at an angle ϑ with the $x-$ axis. The Reynolds number is very small since the induced magnetic field is considered insignificant compared to the applied magnetic field. The effects of the effective Prandtl number, Hall, Soret and Dufour number are significant and thus cannot be ignored. Under these stated assumptions and the usual electromagnetic Boussinesq approximations the governing boundary layer equations are (see [5], [28])

$$\frac{\partial u}{\partial x} + \frac{\partial v}{\partial y} = 0, \tag{1}$$

$$u\frac{\partial u}{\partial x} + v\frac{\partial u}{\partial y} = \nu\frac{\partial^2 u}{\partial y^2} \quad - \quad \frac{\sigma B_o{}^2 \sin^2 \vartheta}{(\rho + \rho m^2)}(u + mw) \tag{2}$$
$$+ \; g\beta_t(T - T_\infty)\cos\gamma \quad + \quad g\beta_m(C - C_\infty)\cos\gamma - \frac{\nu}{K}u,$$

$$u\frac{\partial w}{\partial x} + v\frac{\partial w}{\partial y} = \nu\frac{\partial^2 w}{\partial y^2} \quad + \quad \frac{\sigma B_o{}^2 \sin^2 \vartheta(mu - w)}{(\rho + \rho m^2)} \tag{3}$$
$$- \quad \frac{\nu}{K}w,$$

$$u\frac{\partial T}{\partial x} + v\frac{\partial T}{\partial y} = \frac{\kappa}{\rho C_p}\frac{\partial^2 T}{\partial y^2} - \frac{Q_0(T - T_\infty)}{\rho C_p} + \frac{D_m K_t}{c_{st}c_p}\frac{\partial^2 C}{\partial y^2} \tag{4}$$
$$- \frac{\sigma B_o{}^2 \sin^2 \vartheta}{(\rho + \rho m^2)}(u^2 + w^2) - \frac{1}{\rho c_p}\frac{\partial q_r}{\partial y},$$

$$u\frac{\partial C}{\partial x} + v\frac{\partial C}{\partial y} = D_m\frac{\partial^2 C}{\partial y^2} + \frac{D_m K_t}{T_{me}}\frac{\partial^2 T}{\partial y^2}, \tag{5}$$

where u, v and w represents the components of dimensional velocities parallel to the x, y and z axes respectively. T represents the temperature of the fluid and C is the concentration of the fluid, g is the acceleration due to gravity, ν is the kinematic viscosity, β_t denote the coefficient of thermal expansion of the fluid, β_m represents the concentration expansion coefficient, D_m is the mass diffusivity coefficient, B_0 is the constant magnetic field intensity, κ is the thermal conductivity of the fluid, ρ is the density,

c_p denote the specific heat at constant pressure, m denote the Hall parameter, T_{me} is the mean fluid temperature, K_t is the thermal diffusion ratio, c_{st} denote the concentration susceptibility, and Q_0 represents the heat generation.

The appropriate boundary conditions are

$$u = a_0 x, \ w = 0, \ v = v_w, \ C = C_w, \ T = T_w, \ \ at \ y = 0,$$
$$u = w = 0, \ C = C_\infty, \ T = T_\infty, \ \ as \ \ y \to \infty, \quad (6)$$

where a_0 has dimensions $(time)^{-1}$. Using Rosseland approximation the radiant heat flux q_r is written as

$$q_r = -\frac{4\sigma^*}{3K^*}\frac{\partial T^4}{\partial y}, \quad (7)$$

where K^* is the mean absorption coefficient and σ^* is the Stefan-Boltzman constant. Following Shateyi *et al.* [28], T^4 is expanded in Taylor series about T_∞ to give

$$T^4 \approx -3T_\infty^4 + 4T_\infty^3 T. \quad (8)$$

Therefore

$$q_r = \frac{-16\sigma^* T_\infty^{*3}}{3K^*}\frac{\partial^2 T}{\partial y^2}.$$

Equation (4) becomes

$$u\frac{\partial T}{\partial x} + v\frac{\partial T}{\partial y} = \frac{\kappa}{\rho C_p}\frac{\partial^2 T}{\partial y^2} - \frac{Q_0(T - T_\infty)}{\rho C_p} \quad (9)$$
$$+ \frac{D_m K_t}{c_p c_{st}}\frac{\partial^2 C}{\partial y^2} + \frac{\sigma B_o^2 \sin^2 \vartheta}{\rho(1+m^2)}(u^2+w^2) + \frac{16\sigma^* T_\infty^{*3}}{3\rho K^* c_p}\frac{\partial^2 T}{\partial^2 y}.$$

We non-dimensionalize $(1)-(5)$ using the following similarity transformations:

$$\eta = \left(\frac{a_0}{\nu}\right)^{\frac{1}{2}} y, \ \ u = a_0 x f'(\eta), \ \ v = -(a_0 \nu)^{\frac{1}{2}} f(\eta), \ (10)$$
$$w = (a_0 \nu)^{\frac{1}{2}} r(\eta), \ \ \frac{T - T_\infty}{T_w - T_\infty} = \theta(\eta), \frac{C - C_\infty}{C_w - C_\infty} = \phi(\eta),$$

where $f(\eta)$, $\ ,\theta(\eta), r(\eta)$, and $\phi(\eta)$ are the dimensional stream, temperature , micro-rotation and concentration distribution functions, respectively. By substituting (10) into $(1)-(5)$ we get the following non-dimensional, non-linear and coupled ordinary differential equations:

$$f''' - f'^2 + ff'' + G_t\theta\cos\gamma + G_m\phi\cos\gamma$$
$$-\frac{M}{1+m^2}\sin^2\vartheta f' - \frac{Mm\sin^2\vartheta}{(1+m^2)\sqrt{Re}}r - df' = 0, \quad (11)$$

$$r'' + fr' - \left(d + \frac{M\sin^2\vartheta}{1+m^2}\right)r + \frac{Mm\sin^2\vartheta}{1+m^2}f' = 0, \quad (12)$$

$$\frac{1}{P_{ref}}\theta'' + f\theta' + Q\theta + D_n\phi'' + \frac{ME_c\sin^2\vartheta}{1+m^2}f'^2$$
$$+ \frac{ME_c\sin^2\vartheta}{Re(1+m^2)}r^2 = 0, \quad (13)$$

$$\frac{1}{S_c}\phi'' + f\phi' + S_o\theta'' = 0, \quad (14)$$

where the prime $(')$ indicate differentiation with respect to η where $P_{ref} = P_r/(RP_r+1)$ is the effective Prandtl

number, $P_r = \nu/\alpha$ is the the Prandtl number, $S_o = \frac{D_m K_t a_0}{\nu T_{me}}\frac{(T_w - T_\infty)}{(C_w - C_\infty)}$ is the Soret number, $R = 4\rho T_\infty^3/\kappa K$ is the radiation parameter, $S_c = \nu/D_m$ is the Schmidt number, $D_n = \frac{K_t D_m}{c_{st}c_p\nu}\frac{C_w - C_\infty}{T_w - T_\infty}$ is the Dufour number, $Q = Q_0/c_p a_0$ is the heat generation parameter, $G_t = g\beta_t(T_w - T_\infty)/a_0^2 x$ is the local thermal Grashof number, $G_m = g\beta_m(C_w - C_\infty)/a_0^2 x$ is the local solutal Grashof number, $M = \sigma B_0^2/a_0\rho$ is the magnetic parameter, $Re = a_0 x^2/\nu$ is the Reynolds number, d is the permeability parameter and the Eckert number, $E_c = a_0^2 x^2/c_p(T_w - T_\infty)$. The appropriate boundary conditions are:

$$f(\eta) = F_w, \ f'(\eta) = 1, \ \ \theta(\eta) = 1, \ r(\eta) = 0,$$
$$\phi(\eta) = 1 \ \text{at} \ \ \eta = 0, \quad (15)$$
$$r(\eta) = f'(\eta) = \phi(\eta) = \theta(\eta) = 0, \ \ \text{as} \ \ \eta \to \infty,$$

where the mass transfer coefficient $F_w = -v_w/\sqrt{a_0\nu}$ and $F_w > 0$ denotes blowing and $F_w < 0$ denote suction.

III. METHOD OF SOLUTION

The coupled ODE's (11)-(14) together with the boundary conditions (15) are solved using MATLAB package **bvp4c**. We let

$$\frac{df}{d\eta} = y_2,$$
$$\frac{d^2 f}{d\eta^2} = y_3,$$
$$y_3' = y_2^2 + \left(d + \frac{M}{1+m^2}\sin^2\vartheta\right)y_2 + \frac{Mm\sin^2\vartheta}{(1+m^2)\sqrt{Re}}y_4$$
$$- y_1 y_3 - G_t\cos\gamma y_6 - G_m\cos\gamma \ y_8,$$
$$\frac{dr}{d\eta} = y_5,$$
$$y_5' = \left(d + \frac{M}{1+m^2}\sin^2\vartheta\right)y_4 - y_1 y_5 - \frac{Mm}{1+m^2}\sin^2\vartheta\sqrt{Re} \ y_2,$$

$$\frac{d\theta}{d\eta} = y_7,$$
$$y_7' = \frac{-P_{ref}}{1 - P_{ref}D_n S_c S_o}(y_1 y_7 + Qy_6 - D_n S_c y_1 y_9)$$
$$+ \frac{-P_{ref}}{1 - P_{ref}D_n S_c S_o}\left(\frac{ME_c}{1+m^2}y_2^2 + \frac{ME_c}{(1+m^2)Re}y_4^2\right),$$
$$\frac{d\phi}{d\eta} = y_9$$
$$y_9' =$$
$$\frac{-S_c y_1 y_9 + P_{ref}S_c S_o\left(y_1 y_7 + Qy_6 - \frac{ME_c}{1+m^2}\left(y_2^2 + \frac{y_4^2}{Re}\right)\right)}{1 - S_c S_o D_n P_{ref}}, \quad (16)$$

with the following corresponding conditions:

$$y_1 = F_w, \ y_2 = 1, \ \ y_4 = 0, \ y_6 = 1, \ y_8 = 1, \ \text{at} \ \eta = 0$$

$$y_2 = 0, \ \ y_4 = 0, \ \ y_6 = 0, \ \ y_8 = 0, \ \text{as} \ \eta \to \infty \quad (17)$$

To guarantee that the numerical solutions approach the asymptotic values appropriately, we set $\eta_{max} = 6$. More elaborate information on the method of solution can be found in [13], [28] and references therein.

IV. RESULTS AND DISCUSSION

The problem of effective Prandtl number, Hall currents, aligned magnetic field on MHD fluid flow over an inclined plane in the presence of heat generation, Dufour and Soret effects are reported. The results of numerical calculations for the distribution of the tangential velocity, lateral velocity, temperature and concentration within the boundary layer are discussed. Additionally, the impact of the different parameters that include, effective Prandtl number (P_{ref}), magnetic field inclination angle, (ϑ), flow surface inclination angle (γ), magnetic parameter (M), Hall parameter m, thermal Grashof (G_t), solutal Grashof number (G_m), the Dufour parameter, (D_n), Soret parameter (S_o), and heat generation parameter (Q) on the profiles of velocity, temperature, and concentration are also examined and analysed. A comparison between the present results and earlier work by Shateyi *et al* [28] and Elgazery [12] is drawn and the results are depicted in Table 1. It is deduced that there is excellent agreement between the results of this study and those obtained by Elgazery [12] and Shateyi *et al* [28].

Table 1: The skin friction values obtained using current method compared to results of Elgazery [12] and Shateyi [28] for $M = 1, F_w = -0.7, M = 1, m = G_t = G_m = \gamma = \vartheta = Q = 0.$

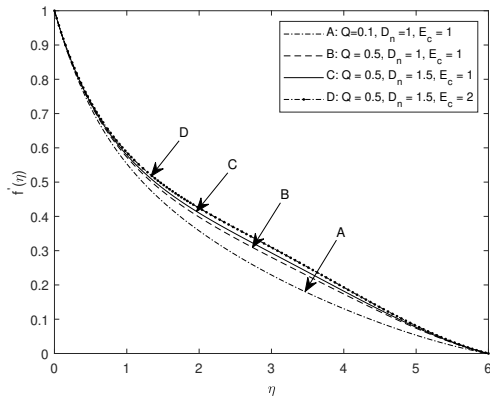| d	Elgazery [12]	Shateyi [28]	Present
1	1.41706	1.41706	1.41706
0.5	1.26942	1.26941	1.26941
0.2	1.17398	1.17398	1.17398
0.1	1.14081	1.14081	1.14081

Figure 2: The effect of Q, D_n and E_c on the tangential velocity with $P_{ref} = 0.23$, $m = M = 1$, $Re = 1$, $\vartheta = 90, \gamma = 0$, $G_t = G_m = 1$, $S_c = 1, S_o = 1$, $d = 1$, $F_w = -0.7$.

The influence of the effective Prandtl number on the tangential velocity profile is displayed in Figure 4. The results show that increasing the effective Prandtl number has the effect of increasing the tangential velocity profile throughout the boundary layer region for effective Prandtl number greater than unity. However, if the value of the effective Prandtl number is less than unity, the velocity profile is raised with enlargement of the effective Prandtl number closer to the wall and experiences a reversed effect further away from the wall. The effects of m, M, γ, and ϑ on the tangential velocity profile is revealed

by Figure 5. It is revealed that the tangential velocity profile declines as the parameters M, γ, and ϑ grow and rises as the Hall parameter is magnified. These results agree with expectations that presence of a magnetic field in an electrically conducting fluid introduces Lorentz force which retards the fluid motion. Also, increasing ϑ retards the tangential velocity. When $\vartheta = 0$, the magnetic field is aligned with the flow direction which assists the fluid motion. The resistance to fluid flow increases as ϑ increases and is optimal when $\vartheta = 90^0$, i.e. when the magnetic field is normal to the flow direction. Similarly, increasing the slope of the flow surface retards the fluid motion. Furthermore, the velocity is maximum when the flow surface is vertical i.e. when $\gamma = 0$ and least when the flow surface is horizontal $(\gamma = 90^0)$. Thus, increasing the angle of inclination of the flow surface γ has the effect of reducing the bouyancy force. Also observed is that increasing the Hall parameter value magnifies the tangential velocity profile.

Figure 2 portrays the effects of the Q, D_n and E_c on the tangential velocity profile. It is evident that the tangential velocity profile is enhanced with increase in the heat generation parameter, Dufour parameter and Eckert number. However, the tangential velocity profile declines with increasing values of the Soret parameter as shown in Figure 3.
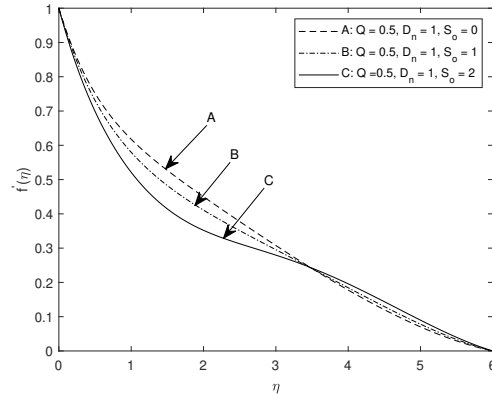

Figure 3: The effect of S_o on the tangential velocity with $D_n = m = M = d = S_c = Re = 1$, $P_{ref} = 0.23$, $\vartheta = 90, \gamma = 0$, $G_t = G_m = 1$, $Q = 0.5$, $F_w = -0.7$.
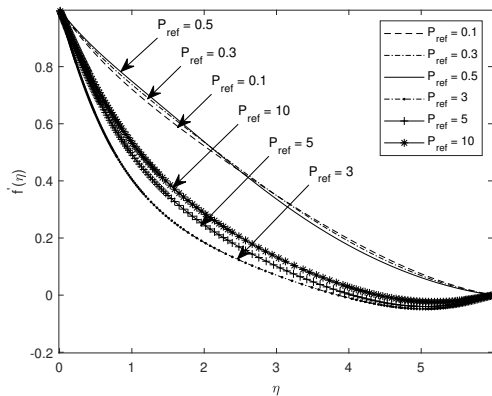

Figure 4: The effect of P_{ref} on the tangential velocity profile with $Q = 0.1$, $G_t = G_m = D_n = m = M = Re = 1$, $\vartheta = 90$, $\gamma = 0$, $S_c = 0.22$.
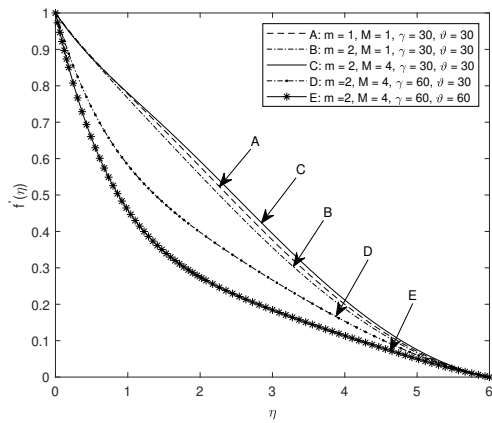
Figure 5: The effect of m, M, ϑ and γ on the tangential velocity profile with $Q = 0.1$, $D_n = 1$, $G_t = G_m = 1$, $\vartheta = 90$, $P_{ref} = 0.23$, $S_c = 0.22$, $Re = 1$.

The effects of S_c, G_t and G_m on the tangential velocity profile is depicted in Figure 6. Also noted is that increasing G_t and G_m simultaneously, amplifies the tangential velocity profile due to buoyancy force enhancement. However, the tangential velocity profile decreases with increasing Schmidt number. Figure 7 exhibits the relationship between the tangential velocity and inclination angles ϑ and γ. It is seen that the profile of the tangential velocity is large when both γ and ϑ are small but minimal if both γ and ϑ are large. For any given combination of the inclinations angles γ and ϑ, the profile is more pronounced if $\vartheta \geq \gamma$. The tangential velocity profile is maximal when $\vartheta = \gamma = 0$ and minimal when $\vartheta = \gamma = 90^0$. The impact of M, D_n and m on the lateral velocity is exhibited in Figure 9. It is observed that the lateral velocity profile increases as D_n and m increase and diminishes as M is increased. Figure 11 displays the effects of the inclinations angles γ and ϑ as well as the Soret parameter on the lateral velocity profile. It is clear from the Figure that the velocity profile is enhanced as S_o increases. Furthermore, it is evident from the Figure that the lateral velocity declines with increase in γ and ϑ. Figure 8 exhibits the role of the suction parameter F_w on the tangential velocity distribution. It clear from the Figure that the tangential velocity profile diminishes as the suction parameter is amplified.

The effect of Q, D_n, and S_o on the temperature distribution is illustrated in Figure 15. The Figure reveals that the temperature profile is enhanced with the rise in the values of the param-
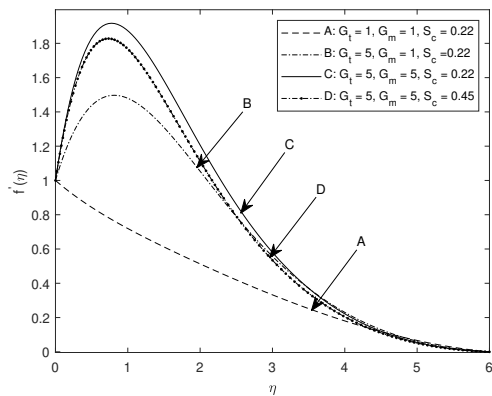

Figure 6: The influence of G_t, G_m and S_c on the tangential velocity with $Q = 0.1$, $D_n = m = M = Re = 1$, $\vartheta = 90$, $P_{ref} = 0.23$, $\vartheta = 90$, $\gamma = 0$.
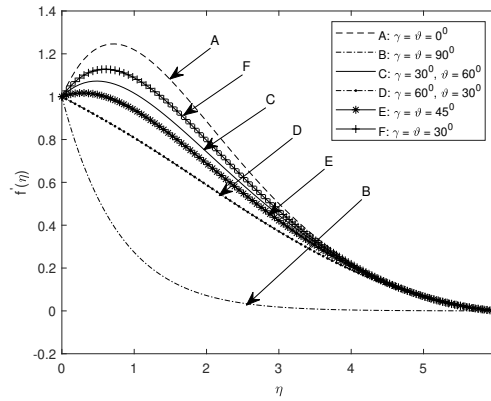

Figure 7: The effect of S_o, γ and ϑ on the tangential velocity with $Q = 0.1$, $m = M = D_n = m = Re = 1$, $P_{ref} = 0.23$, $G_m = G_t = 2$, $S_c = 0.22$.
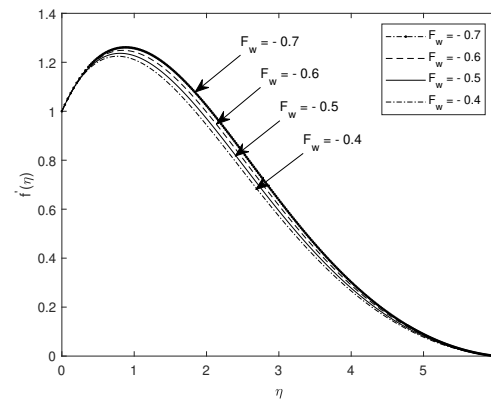

Figure 8: The effect of F_w on the tangential velocity with $m = D_n = M = Re = S_o = 1$, $Q = 0.5$, $\vartheta = 90$, $\gamma = 0$, $P_{ref} = 0.23$, $S_c = 0.22$, $Gm = G_t = 2$.

eters Q, D_n and S_o. Figure 16 exhibits the impact of P_{ref} on the temperature distribution. From the Figure, it is observed that for values of $P_{ref} < 1$ the temperature profile increases as P_{ref} increases closer to the wall and has reverse effect further away from the wall. However for $P_{ref} > 1$ the temperature profile increases as P_{ref} increases. The effective Prandtl number effect on the lateral velocity is depicted in Figure 12. The Figure clearly shows that the lateral velocity diminishes with rising P_{ref} values for values of $P_{ref} \leq 1$ and increases with increasing effective Prandtl number for values of $P_{ref} > 1$. Figure 14 illustrates the the effect of S_c, G_m, G_t and E_c on the lateral velocity. It is revealed that the value of the lateral velocity rises with enlargement of of the parameters G_m, G_t and E_c and diminishes when S_c is magnified.

The impact of permeability parameter d on the profiles of the tangential velocity, lateral velocity, temperature, and concentration is demonstrated in Figures 10, 13, 20 and 25 respectively. Evidence from the graphs show that as d increases the velocity and temperature profiles are reduced. On the other hand, the concentration profile is magnified as d increases. The thickness of the boundary layer diminishes with increasing value of the permeability parameter which results in more fluid leaving boundary layer surface as the tightness of the porosity is reduced.

Figure 18 displays the effect of S_c, G_m, G_t on the temperature profile. The temperature profile is enlarged as the parameter S_c increases. Also noticed is that the temperature profile is

enhanced as G_t and G_m increase for $\eta < 2$ with reversed effect for $\eta > 2$. Figure 19 illustrates the influence of the Eckert number on the temperature profile. The Figure reveals that the temperature profile grows as the Eckert number increases. The influence of Q, S_o and D_n on the concentration distribution is manifested clearly in Figure 21. As expected, the concentration profile decreases as S_0, D_n and Q increase. Figure 17 presents the effects of m, M, γ, ϑ on the temperature profile. According to the graph, the temperature profile increases as M and γ increase and decreases as m and ϑ increase. Figure 22 displays

Table 2: The effect of M, m, ϑ, γ and P_{ref} on the mass transfer rate $-\phi'(0)$, heat transfer rate $-\theta'(0)$ and skin friction coefficient $-f''(0)$ with $G_t = 5$, $G_m = 1$, $Q = 1$, $Re = 1$, $S_c = 0.22$, $S_o = 0$, $d = 1$, $E_c = 1$, $r = 0.1$

m	M	ϑ	γ	P_{ref}	$-f''(0)$	$-\theta'(0)$	$-\phi'(0)$
3	1	30	30	0.3	-1.7140	-0.5297	-0.0310
3	1	80	80	0.3	0.8344	0.6336	0.1253
3	1	30	60	0.3	-0.0992	0.3538	0.1468
3	1	60	30	0.3	-1.1773	-0.0147	0.0991
3	1	80	90	0.3	1.1444	5.4450	0.1614
3	1	90	80	0.3	0.8343	0.5940	0.1041
3	2	90	80	0.3	0.8713	0.6423	0.1380
2	1	60	30	0.3	-0.7673	0.3824	0.2587
2	1	60	30	0.4	-1.0108	0.0630	0.2063
2	1	30	60	0.3	-0.0417	0.2983	0.1477

the effects of m, M, G_t and G_m on the concentration profile. It is revealed that the fluid concentration profile decreases as G_t and G_m increase. On the contrary, the concentration profile is magnified as m and M are enlarged. Figure 23 shows that as γ and ϑ increase, the concentration profile also increases. On the other hand, the concentration profile declines with increase in the values of the parameters S_c and E_c. The relationship between the effect of P_{ref} and concentration is conveyed by Figure 24. The graph shows that for values of $P_{ref} < 1$ the concentration profile decreases as P_{ref} increases closer to the wall and has reverse effect further away from the wall. However, for $P_{ref} > 1$ the concentration profile increases as P_{ref} increases. The effect of m, M, ϑ, γ, P_{ref}, d, Q, D_n, G_t, G_m, E_c and S_o on the mass transfer rate $-\phi'(0)$, heat transfer rate $-\theta'(0)$ and skin friction $-f''0$ are displayed in Tables 2, 3 and 4. It is established that the skin friction increases as γ, ϑ, M, d, D_n, G_t, G_m, E_c increase and decreases as P_{ref}, m, Q, S_c, and S_o increase. It is also deduced that heat transfer rate is enhanced
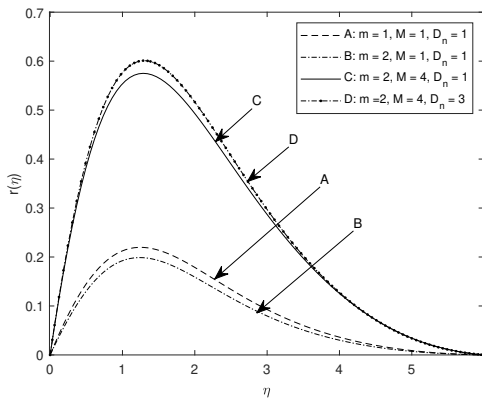
Figure 9: Lateral velocity profile for varying values of m, M and D_n with $Q = 0.5$, $D_n = 1$, $m = M = 1$, $P_{ref} = 0.23$, $G_m = G_t = 2$, $S_c = 0.22$, $Re = 1$.
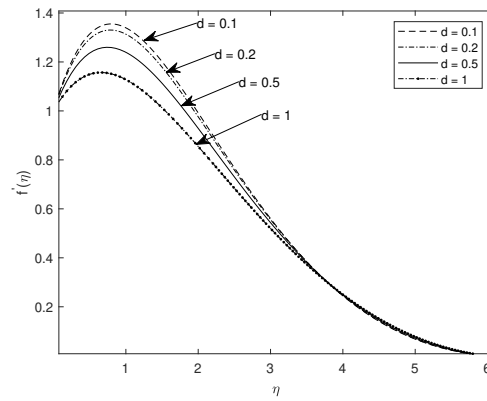
Figure 10: The effect of d on the tangential velocity with $Q = 0.5$, $m = D_n = M = S_o = Re = 1$, $\vartheta = 90$, $\gamma = 0$, $P_{ref} = 0.23$, $G_m = G_t = 2$, $S_c = 0.22$.
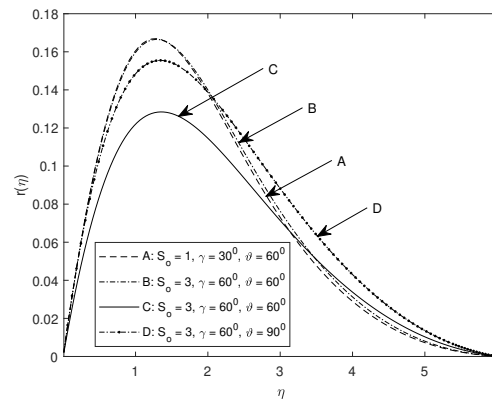
Figure 11: The effect of S_o, ϑ and γ on lateral velocity with $Q = 0.5$, $D_n = m = Re = M = 1$, $P_{ref} = 0.23$, $G_m = G_t = 2$, $S_c = 0.22$.
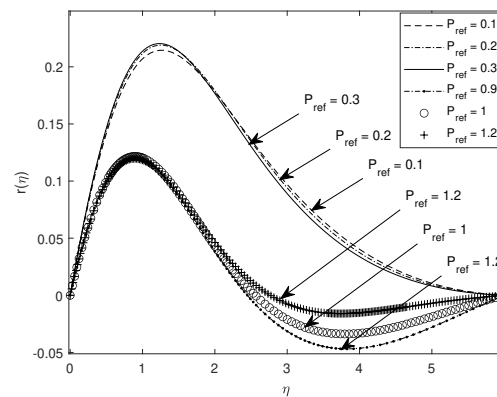
Figure 12: The effect of P_{ref} on the lateral velocity with $Q = 0.5$, $D_n = m = M = Re = 1$, $\vartheta = 90$, $\gamma = 0$, $G_m = G_t = 2$, $S_c = 0.22$.

as γ, ϑ, M, d, D_n, S_c, G_t, G_m, E_c increase and decreases as P_{ref}, S_c and Q increase.

The mass transfer was found to increase as γ, ϑ, M, d, D_n, P_{ref}, S_c, G_t, G_m, E_c and S_o increase and decreases as m and Q increase. It is observed that the values of mass transfer rate, skin friction and heat transfer rate are minimal when both γ and ϑ are smallest and maximal when both γ and ϑ are largest. Furthermore, it is noticed that for any given combination of ϑ and γ the mass transfer rate, heat transfer rate and skin friction
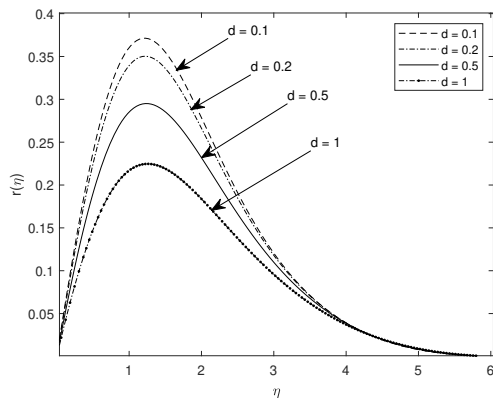
Figure 13: The effect of d on the lateral velocity with $Q = 0.5$, $D_n = m = S_o = M = Re = 1$, $\vartheta = 90$, $\gamma = 0$, $P_{ref} = 0.23$, $G_m = G_t = 2$, $S_c = 0.22$.
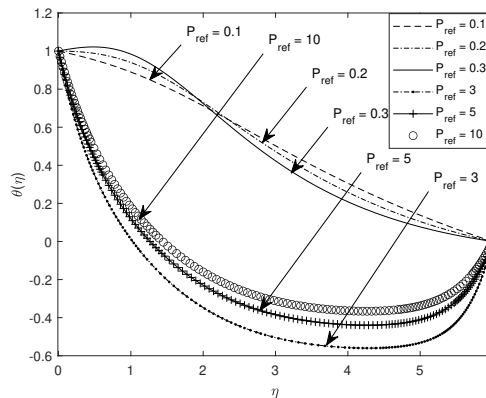

Figure 14: The effect of S_c, G_m, G_t and E_c on the lateral velocity profile with $Q = 0.1$, $D_n = m = S_o = M = Re = 1$, $\vartheta = 90$, $\gamma = 0$, $S_c = 0.22$.

Figure 15: The effect of Q, D_n and S_o on the temperature profile with $m = M = Re = 1$, $G_t = G_m = 2$, $P_{ref} = 0.23$, $\vartheta = 90$, $\gamma = 0$.

Figure 16: The effect of P_{ref} on the temperature profile with $S_o = m = Re = M = 1$, $G_t = G_m = 2$, $Q = 0.1$, $\vartheta = 90$, $\gamma = 0$.
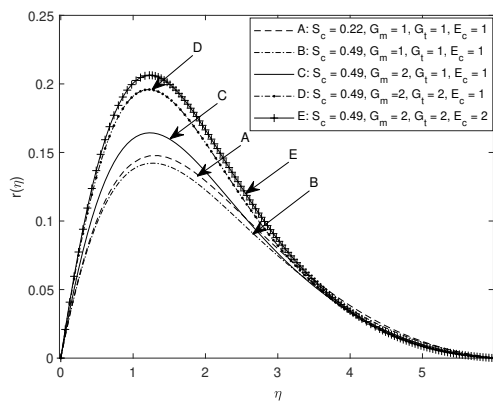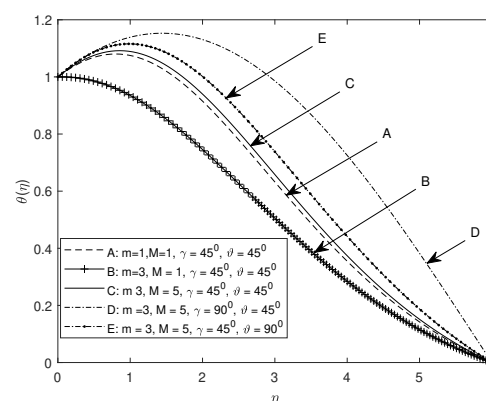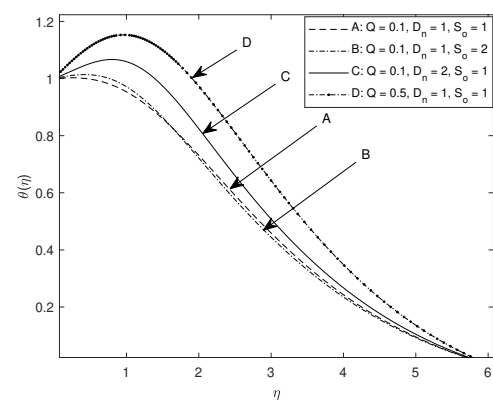

Figure 17: The effect of m, M, ϑ and γ on the temperature profile with $Q = 0.5$, $G_t = G_m = 2$, $P_{ref} = 0.23$, $S_c = 0.22$, $S_0 = D_n = Re = 1$.
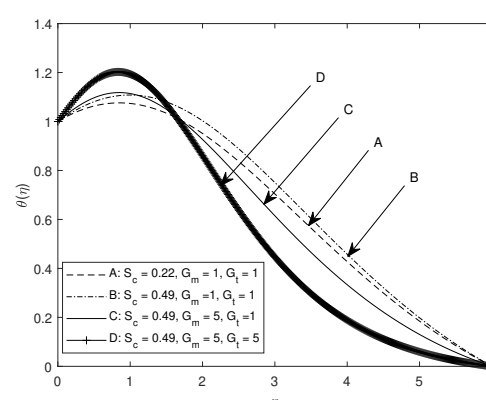

Figure 18: Temperature profile for varying values of S_c, G_m, and G_t with $Q = 0.5$, $m = M = 1$, $P_{ref} = 0.23$, $S_o = 1$, $\vartheta = 90$, $\gamma = 0$, $D_n = 1$, $Re = 1$.

are more pronounced whenever $\gamma > \vartheta$.

V. CONCLUDING REMARKS

The paper investigates the effect of the Soret number, Dufour number, effective Prandtl number, Hall currents on the steady MHD flow past an inclined plane in the presence of variable magnetic field and heat generation. The partial differential equations are reduced to a system of non-linear ordinary dif-

ferential equations by introducing similarity variables. Using MATLAB **bvp4c** calculations are carried out for the various values of the dimensionless parameters considered in this paper. The results of the study are displayed in graphs and tables. The conclusion made is that the tangential velocity, lateral velocity, concentration, temperature, mass transfer rate, heat transfer rate and skin friction are influenced significantly by the different parameters involved in the current study. The present numerical study led to the following deductions.
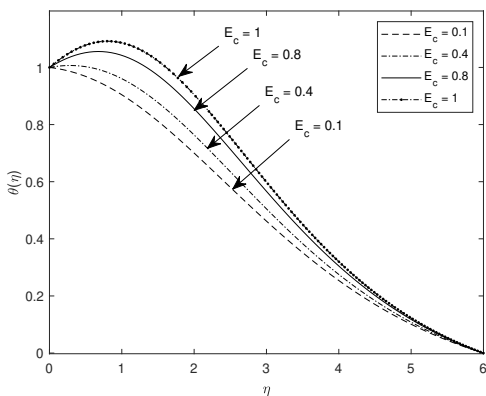
Figure 19: The effect of E_c on the temperature profile with $Q = 0.5$, $D_n = m = Re = M = S_o = 1$, $\vartheta = 90$, $\gamma = 0$, $P_{ref} = 0.23$, $G_m = G_t = 2$, $S_c = 0.22$.
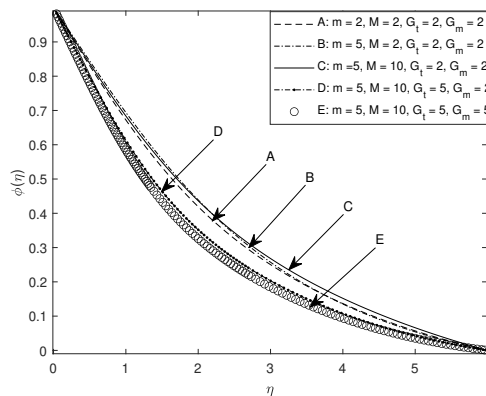

Figure 22: The effect of m, G_t, M and G_m on the concentration profile with $Q = 0.5$, $P_{ref} = 0.23$, $S_c = 0.22$, $\vartheta = 90$, $\gamma = 0$, $D_n = Re = S_o = 1$.
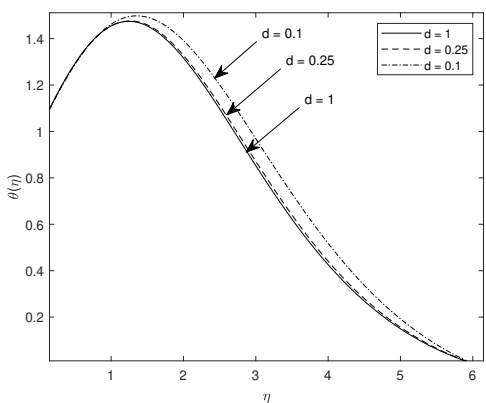

Figure 20: The effect of d on the temperature profile with $D_n = m = S_o = M = Re = 1$, $\vartheta = 90$, $\gamma = 0$, $P_{ref} = 0.23$, $G_m = G_t = 2$, $S_c = 0.22$, $Q = 0.5$.
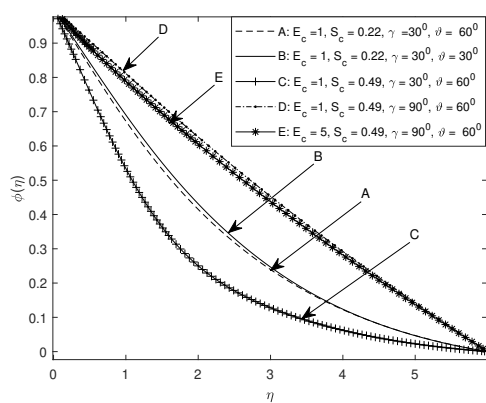

Figure 23: The effect of S_c, γ, ϑ, and E_c on the concentration profile with $Q = 0.1$, $P_{ref} = 0.23$, $\vartheta = 90$, $\gamma = 0$, $D_n = Re = S_o = 1$.
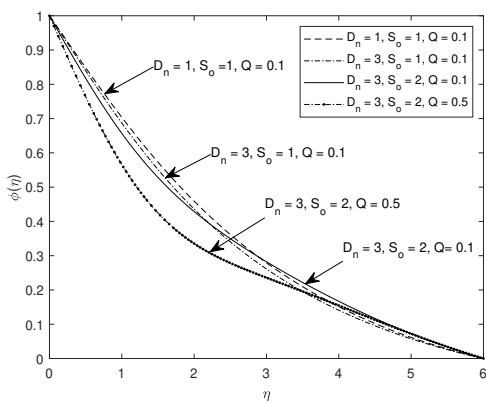

Figure 21: Variation of concentration profile for varying values of D_n, S_o, and Q with $G_t = G_m = 2$, $S_c = 0.22$, $\vartheta = 90$, $\gamma = 0$, $D_n = 1$, $P_{ref} = 0.23$, $Re = 1$.
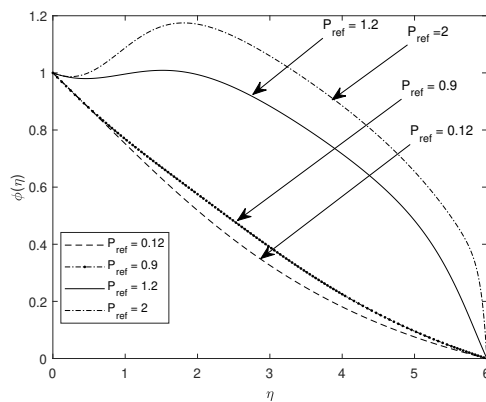

Figure 24: The effect of P_{ref} on the concentration profile with $Q = 0.1$, $D_n = G_t = G_m = m = M = S_o = Re = 1$, $\vartheta = 90$, $\gamma = 0$.

1. The tangential velocity profile increases with increase in the values of d, G_t, G_m, Q, D_n, E_c, m and $P_{ref} < 1$ near the wall and diminishes with enlarged values of M, ϑ, γ, S_c, F_w and $P_{ref} > 1$ further away from the wall.

2. The tangential velocity profile is significantly pronounced when both inclination angles, ϑ and γ are relatively small. However, it is small, if both ϑ and γ are large. For any given combination of ϑ and γ the profile is more pronounced if $\vartheta \geq \gamma$.

3. The lateral velocity profile increases with increase in the values of d, D_n, S_o, G_t, G_m, M, E_c and $P_{ref} > 1$. On the contrary, the lateral velocity declines with enlarged values of the parameters m, γ, ϑ, S_c, G_t, G_m, $P_{ref} > 1$ and $P_{ref} < 1$ near the wall.

4. An increase in d, Q, D_n, M, γ, G_t, G_m, E_c and $P_{ref} > 1$ near the wall causes a rise in the temperature profile. On the contrary, the temperature profile declines with a rise in the value of the parameters S_o, m, ϑ and $P_{ref} < 1$ further
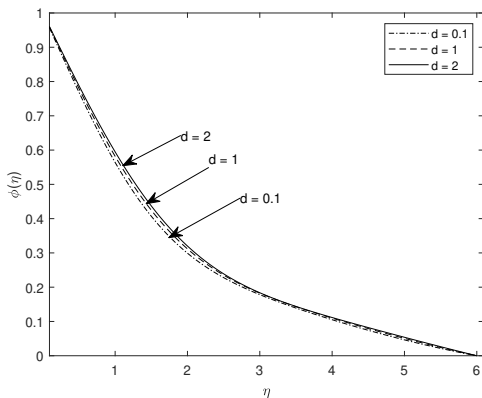
Figure 25: The effect of d on the concentration profile with $Q = 0.1$, $D_n = Re = S_o = 1$.

Table 3: The effect of d, Q, D_n, S_o on the mass transfer rate $-\phi'(0)$, heat transfer rate $-\theta'(0)$ and skin friction coefficient $-f''(0)$ with $G_t = 5$, $G_m = 1$, $m = 2$, $M = 1$, $Re = 1$, $S_c = 0.22$, $E_c = 1$, $r = 0.5$, $P_{ref} = 0.3$

d	Q	D_n	S_o	$-f''(0)$	$-\theta'(0)$	$-\phi'(0)$
0.1	0.5	0.5	0.5	-1.6292	0.2915	0.2131
0.5	0.5	0.5	0.5	-1.0666	0.5696	0.2626
1.0	0.5	0.5	0.5	-1.3003	0.1734	0.0457
1.0	1.0	0.5	0.5	-1.0492	0.3546	0.2780
1.0	2.0	0.5	0.5	-1.5611	-0.2937	0.2624
1.0	2.0	1.0	0.5	-1.5375	-0.2683	0.2911
1.0	2.0	2.0	0.5	-1.5599	0.2992	0.3042
1.0	2.0	2.0	1.0	-1.6574	-0.4341	0.3479
1.0	2.0	2.0	2.0	-1.8105	-0.6776	0.5109

Table 4: The effect of S_c, G_t, G_m, E_c on the mass transfer rate $-\phi'(0)$, heat transfer rate $-\theta'(0)$, skin friction coefficient $-f''(0)$ with $m = 1$, $M = 1$, $Re = 1$, $r = 0.5$, $Q = 0.5$, $d = 1$, $r = 0.5$, $\vartheta = 90$, $\gamma = 0$, $P_{ref} = 0.3$

S_c	G_t	G_m	E_c	$-f''(0)$	$-\theta'(0)$	$-\phi'(0)$
0.22	1.0	1.0	1.0	-0.3116	0.2890	-0.3218
0.49	1.0	1.0	1.0	-0.3334	0.3402	-0.4706
0.49	2.0	1.0	1.0	0.1696	0.3453	-0.5210
0.49	2.0	2.0	1.0	0.5118	0.3571	-0.5434
0.49	2.0	2.0	2.0	0.6015	0.7757	-0.6957

away from the wall.

5. The concentration profile increases as d, m, M, γ, ϑ, $P_{ref} > 1$ and $P_{ref} < 1$ for $\eta < 1.5$. An increase in the values of G_t, G_m, E_c, S_c, D_n, S_o, Q and $P_{ref} < 1$ for $\eta > 1.5$ results in a decrease in concentration profile.

6. The skin friction is enhanced with a rise in the values of the parameters ϑ, γ, M, d and D_n. In contrast, the skin friction diminishes with increase in the values of m, Q and S_o.

7. The rise in the values of ϑ, γ, M, d and D_n enhances the heat transfer rate. Conversely, it decreases as P_{ref}, S_c and Q increase.

8. The mass transfer rate increases with increasing values of ϑ, γ, M, d $Pref$ S_o and D_n. However, it reduces as m and Q increase.

Most of the above findings on the effect of the various parameters on fluid flow agree with previous publications. Most outstanding findings in this investigation are that for optimal velocity profile the angles of inclination ϑ and γ need be relatively small and for any given combination $\vartheta \geq \gamma$. Furthermore, minimal values of the mass transfer rate, heat transfer rate and the skin friction coefficient are obtained when both γ and ϑ are smallest and maximal when both angles are largest. For any given combination of γ and ϑ the effect is more pronounced whenever $\gamma \geq \vartheta$. The effect of the effective Prandtl number depends on whether its value is greater or less than unity. In all cases, $0 \leq R < 1$ and $P_r > R$.

REFERENCES

[1] E. M. Abo-Eldanab, A. M. Salem, "Hall effects on MHD free convection flow of a non-Newtonian power law fluid at a stretching surface", Int. Commun. Heat Mass Transfer, vol. 31, no. 3, pp. 343, 2004.

[2] N. Acharya, S. Maity, P. K. Kundu, "Influence of inclined magnetic field on the flow of condensed nanomaterial over a slipping surface:the hybrid visualization", Applied Nanoscience, vol. 10, pp. 633-647, 2020.

[3] M. S. Alam, M. M. Rahman and A. Satter, "Effects of variable suction and thermophoresis on steady MHD combined free-forced convective heat and mass transfer flow over a semi-infinite permeable inclined plate in the presence of thermal radiation", Int. J. Therm. Sci., vol. 47, no. 6, pp. 758-765, 2008.

[4] M. S. Alam, M. M. Rahman and A. Satter, "Transient magnetohydrodynamic free convective heat and mass transfer flow with thermophoresis past a radiate inclined permeable plate in the presence of variable chemical reaction and temperature dependent viscosity", Nonlinear Analysis: Model Control, vol. 14, pp. 3-20, 2009.

[5] M. Ali, M. S. Alam, M. M. Alam, M. A. Alam, "Radiation and thermal diffusion effect on a steady MHD free convection heat and mass transfer flow past an inclined stretching sheet with Hall current and heat generation", IOSR Journal of mathematics, vol. 9, no. 4, pp. 33-45, 2014.

[6] G. Buzuzi, J. B. Munyakazi and K. C. Patidar, "A fitted numerical method to investigate the effect of various parameters on an MHD flow over an inclined plate", Numer. Methods for Partial Diff. Equations, DOI 10.1002/num, pp. 107-120, 2015.

[7] G. Buzuzi and A. N. Buzuzi, "Unsteady MHD convection flow and heat transfer past a vertical inclined plate in a porous medium with variable plate temperature with suction in a slip flow regime", Int. J. of Appl. Math., DOI: 10.12732/ijam.v32i2.4, vol. 32, no. 2, pp. 205-218, 2019.

[8] G. Buzuzi, A. N. Buzuzi, T. Nyamayaro, W. Manamela, K. S. Ramolotja, "The study of magneto hydrodynamic free convective flow and heat transfer in a porous medium with heat generation, radiation absorption and chemical reaction", Int. J. of Appl. Math., DOI: 10.12732/ijam.v33i4.15, vol. 33, No 4, pp. 733-756, 2020.

[9] G. Buzuzi, "Inclined magnetic field and effective Prandtl number effects on unsteady MHD oscillatory flow past an inclined surface with constant suction and chemical reaction", Journal of the Nigerian mathematical Society, vol. 40, no. 3, pp.227-244, 2021.

[10] T. G. Cowling, "Magnetohydrodynamics", Interscience Publishers, New York, 1957.

[11] R. Devi, V. Poply, Manimala, "Effects of aligned magnetic field and inclined outer velocity in Casson fluid flow over a stretching sheet with heat source", Journal of Thermal Engineering, vol. 7, no. 4, pp. 823-844, 2021.

[12] N. S. Elgazery, "The effects of chemical reaction, Hall and ion-slip currents on MHD fow with temperature dependent viscosity and thermal diffusivity", Communications in Nonlinear Science and Numerical Simulations, vol. 14, no. 4, pp. 1267-1283, 2009.

[13] N. Gajjela, A. Matta, K. Kaladhar, "The effects of Soret and Dufour, chemical reaction, Hall and ion currents on magnetized micropolar flow through co-rotating cylinders", AIP ADVANCES, vol. 7, no. 11, 2017.

[14] F. S. Ibrahim, A. M. Elaiw and A. A. Bakr, "Effect of the chemical reaction and radiation absorption on the unsteady MHD free convection flow past a semi infinite vertical permeable moving plate with heat source and suction", Commun. in Nonlin. Sci. and Numer. Simul., vol. 13, pp. 1056-1066, 2008.

[15] M. V. Kishna, K. Jyothi, "Hall effect on MHD rotating flow of a visco-elastic fluid through a porous medium over an infinite oscillating porous plate with heat source and chemical reaction", Mater. Today: Proc, vol. 5, pp. 367-380, 2018.

[16] M. V. Krishna, B. V. Swarnalathamma, A. J. Chamka, "Investigations of Soret, Joule, and Hall effects on MHD rotating mixed convective flow past an infinite vertical porous plate", Journal of Ocean Engineering and Science, vol. 4, pp. 263-275, 2019.

[17] E. Mgyari, "Comment on "Mixed convection boundary layer flow over a horizontal plate with thermal radiation" by A Ishak, Heat mass Transfer, DOI 10.1007/s00231-009-0552-3", Heat Mass Transfer, vol. 46, pp. 509-810, 2010.

[18] E. Magyari, A. Pantokratoras, "Note on the effect of thermal radiation in the linearized Roseland approximation on the heat transfer characteristics of various boundary layer flows", International Communications in Heat and Mass Transfer, vol. 38, pp. 554-556, 2011.

[19] U. S. Rajput, Neetu Kamaijia, "MHD flow past a vertical Plate with variable temperature and mass diffusion in the presence of Hall current", International Journal of Applied Science and Engineering, vol. 14, no. 2, pp. 115-123, 2016.

[20] C. S. K. Raju, N. Sandeep, C. Sulochana, V. Suganamma and M. Jayachandra, "Radiation, inclined magnetic field and cross-diffusion effects on flow over a stretching surface", Journal of the Nigerian Mathematical Society, vol. 34, pp. 169-180, 2015.

[21] G. S. Reddy, S. K. Reddy, P. D Prasad, S. V. Varma, "Diffusion-thermo and aligned magnetic field effects on force convection on flow past an inclined porous plate with first order chemical reaction", IOSR Journal of Electrical and Electronics Engineering, vol. 12, no. 3, pp. 25-33, 2017.

[22] P. Roja, T. S. Reddy and N. B. Reddy, "Double diffusive convection-radiation interaction on unsteady Mhd flow of a micropolar fluid over a vertical moving porous plate embedded in a porous medium with heat generation and soret effects", Int. J. of Engin. and Sci., vol. 1, no. 2. pp. 201-214, 2012.

[23] M. J. Sabhakar, K. Gangadhar, N. B. Reddy, "Soret and Dufour effects on MHD convective flow of and mass transfer over a moving non-isothermal vertical plate with heat generation/absorption", Advances in Applied Science Research, vol. 3, no. 5, pp. 3165-3184, 2012.

[24] S. O. Salawu and M. S. Dada, "Radiation heat transfer of variable viscosity and thermal conductivity effects on inclined magnetic field with dissipation in a non-Darcy medium", Journal of the Nigerian mathematical Society, vol. 35, pp. 93-106, 2016.

[25] A. M. Salem, M. Abd El Aziz, "Effect of Hall currents and chemical reaction on hydromagnetic flow of a stretching vertical surface with internal heat generation/absorption", Applied Mathematical Modelling, vol. 32, pp. 1236-1254, 2008.

[26] N. Sandeep and V. Sugunamma, "Radiation and inclined magnetic field effects on unsteady hydromagnetic free convection flow past an impulsively moving vertical plate in a porous medium", J. Appl. Fluid. Mech., vol. 7, no. 2, pp. 275-286, 2014.

[27] M. A. Seddeek, M. S. Abdelmeguid, "'Effects of radiation and thermal diffusivity on heat transfer over a stretching surface with variable heat flux", Physics Letters A, vol. 348, no. 36, pp. 172-179, 2006.

[28] S. Shateyi, S. S. Motsa, P. Sibanda, "The effects of Thermal Radiation, Hall currents, Soret, and Dufour on MHD Flow by Mixed Convection Over a Vertical Surface in Porous media", Mathematical Problems in Engineering, vol. 2010, Article ID 627475, 20 pages, 2010.

[29] M. Shoaib, T. Rafia, M. A. Z. Raja, W. A. Khan, M. Waqas, "Further analysis of double - diffusive flow of nanofluid through a porous medium situated on an inclined plane: AL-based Levenberg-Marquardt scheme with back propagated neural network", Journal of the Brazilian Society Mechanical Sciences and Engineering, https//doi.org/10.100/s40430-022-03451-9, vol. 44, no. 227, 2022.

[30] T. Srinivasulu, B. S. Goud, "Effect of inclined magnetic field on flow, heat and mass transfer of Williamson nanofluid over a stretching sheet", Case Studies in Thermal Engineering, https://doi.org/10.1016/csite.2020.100819, vol. 23, 2021.

[31] C. Sivaraj, M. A. Sheremet, "MHD natural convection in an inclined square porous cavity with a heat conducting solid block", Journal of Magnetism and Magnetic materials, vol. 426, pp. 351-360, 2017.

[32] L. S. R. Titus, A. Amamma, T. K. Screelakshmi, A. S. Chethan, "Ferromagnetic liquid flow due to inclined stretching of an elastic sheet," Lecture Notes in Engineering and Computer Science: Proceedings of the World Congress Engineering 2018, WCE 2018, 4-6 July, 2018, London, U.K., pp 44-49.

[33] M. J. Uddin, "Convective flow of micropolar fluids along an inclined flat plate with variable electric conductivity and uniform surface heat flux", DAFFODIL Int. Univ. J. of Sci. and Techn., vol. 6, no. 1, pp. 69-79, 2011.

[34] T. Pop, "Hall effects on magneto-hydrodynamic boundary layer flow over a continuous moving flat plate", Acta Mech, vol. 108, no. 1, 1995.

[35] R. Vijayaragavan, M. Ramesh, S. Karthikayan, "Heat and mass transfer investigation on MHD Casson fuid flow past an induced porous plate in the effects of Dufour and chemical reaction", Journal of Xi'an University of Archtecture and Technology", vol XIII, no. 6, 2021.